



**HAL**  
open science

## On residual stress development during gaseous nitriding of M2 steel

Yanxue Zhang, Sébastien Jégou, Laurent Barrallier, David Mercs

► **To cite this version:**

Yanxue Zhang, Sébastien Jégou, Laurent Barrallier, David Mercs. On residual stress development during gaseous nitriding of M2 steel. ICRS 11 - The 11th International Conference of Residual Stresses, SF2M; IJL, Mar 2022, Nancy, France. hal-03791325v1

**HAL Id: hal-03791325**

**<https://hal.univ-lorraine.fr/hal-03791325v1>**

Submitted on 29 Sep 2022 (v1), last revised 6 Oct 2022 (v2)

**HAL** is a multi-disciplinary open access archive for the deposit and dissemination of scientific research documents, whether they are published or not. The documents may come from teaching and research institutions in France or abroad, or from public or private research centers.

L'archive ouverte pluridisciplinaire **HAL**, est destinée au dépôt et à la diffusion de documents scientifiques de niveau recherche, publiés ou non, émanant des établissements d'enseignement et de recherche français ou étrangers, des laboratoires publics ou privés.



Distributed under a Creative Commons Attribution - ShareAlike 4.0 International License

# On residual stress development during gaseous nitriding of M2 steel

Yanxue Zhang<sup>a,b,\*</sup>, Sébastien Jégou<sup>a</sup>, Laurent Barrallier<sup>a</sup> and David Mercs<sup>b</sup>

<sup>a</sup>*MSMP laboratory, Arts et Metiers Institute of Technology, 2 cours des Arts et Métiers, 13617, Aix-en-Provence, France.*

<sup>b</sup>*Department of Research Innovation Expertise, Lisi-automotive, 2 rue Juvénal VIELLARD, 90600, Grandvillars, France.*

---

## ABSTRACT

Due to phase transformation, the residual stress evolution is deeply dependent on chemical and thermodynamical reactions during gaseous nitriding. This work will present and analyze the residual stress profiles in M2 high-speed steel samples with different gas nitriding parameters (temperatures, nitriding times, nitriding potentials). The relations of residual stress, hardness, and the corresponding chemical composition profile are studied.

**Keywords:** Residual stress, Phase transformation, Gaseous nitriding, M2 steel, Hardness

---

## 1. Introduction

High-speed steels are always subjected to high pressure or high shear working conditions as forming tools, the high hardness and compressive residual stresses are required to improve the wear resistance and the fatigue life of the tools [1-3]. Nitriding is a thermochemical treatment based on the diffusion of nitrogen that is often used to modify the mechanical properties in the surface layer [4]. The hardness gradient in the nitriding layer is generally inconsistent with the nitrogen concentration gradient of which the maximum is at the surface [5]. But the residual stress evolution is more complicated during nitriding, the maximum value is often in-depth due to the carbon redistribution and grain coarsening [6]. So, it is with great importance to understand how the residual stress evolves in the material during nitriding to achieve an optimized mechanical profile.

Origins of residual stresses during nitriding have been attributed to volume changes caused by the precipitation of nitrides and phase transformation of initial carbides [1,4,7]. An in-depth gradient of residual stresses develops below the surface with the composition gradient. In the case of M2 steel, alloy elements (Cr, Mo, V, W) form nitrides with nitrogen diffused in the material and participate in the phase transformation between the carbides and nitrides [3]. The

---

\* Corresponding author. yanxue.zhang@ensam.eu

transformation of carbides and carbon co-diffusion decreases nitriding kinetics and impacts residual stress [6,8].

## 2. Experiments

### 2.1. Material and sample preparation

AISI M2 steel was hardened and tempered with a final hardness of  $763 \pm 35$  HV0.2. The chemical composition was measured as shown in Table 1. Samples with dimensions  $17 \times 13 \times 5$  mm<sup>3</sup> were nitrided in a thermogravimetric analyzer Setsys Evolution ATG-ATD/DSC from SETARAM Instrumentations. The nitriding temperatures are 500 and 540 °C, nitriding potential varies from 0.5 to 3.7 atm<sup>-1/2</sup>, nitriding time is from 5 hours to 15 hours.

Table 1: Chemical composition of M2 steel samples (wt.%).

C	W	Mo	V	Cr	Si	Co	Mn	N
0.884	6.352	4.513	1.729	3.807	0.306	0.372	0.271	0.025

### 2.2. Characterization methods

A JEOL 7001F microscope, equipped with an Oxford Instrument INCA energy-dispersive X-ray detection system (EDX) have been used for observation and local chemical analysis. Back-scattered electrons (BSE) mode with EDX technic was applied for phase analysis. The observation was performed with an accelerating voltage of 12 kV.

The concentrations of nitrogen and carbon were measured using an optical emission spectrometer with Spectromax BT MX5M from Ametek. The in-depth concentration analyses are carried out by successive measurements at depths reached by grinding with a SiC disk of 120 grade to remove about 25 µm thickness after each series of measures. The result gives the mean value of all the removed material of four tests at each depth.

The micro-hardness was measured with Q10A+ from Qness indentation device with the help of the programming function of the software QpixControl2. The load of 2 N worked on the sample surface for 10 seconds during the measurement. Three tests were performed at each equivalent area on a mirror-polished surface.

The residual stress analyses were performed on a Siemens D500 diffractometer, equipped with a linear detector from Elphyse, a chromium anode  $\lambda_{k\alpha} = 0.2291$  nm and a vanadium filter. The  $\sin^2\psi$  method was used for stress measurement on the family of {211} planes of the ferrite. The analysis is performed using 13 angles, including an oscillation of  $\pm 3^\circ$  and an acquisition time of 100 s. The X-ray elastic constant were calculated from ferritic elasticity constants (Young module  $E = 210$  GPa, Poisson ratio  $\nu = 0.29$ , anisotropy factor  $ARX = 1.39$ ) and Kröner-Eshelby type model ( $1/2 S_2 = 5.81 \times 10^{-6}$  MPa<sup>-1</sup>,  $S_1 = -1.27 \times 10^{-6}$  MPa<sup>-1</sup>). The in-depth profile below the surface was reached by successive electrochemical polishing (Struers Lectropol 5, with electrolyte A2) using a depth increment of 20 µm measured by an electronic micrometer.

## 3. Results and discussions

### 3.1. Nitriding time

Fig.1. (a) shows the chemical profiles of nitrogen and carbon from the surfaces to in-depths of the three samples nitrided for 5 and 15 hours respectively at 500 °C,  $K_N = 1$  atm<sup>-1/2</sup>. As the

nitriding time increases, nitrogen diffuses deeper. The maximum nitrogen concentration near the surface is about the same. Carbon accumulates at the nitrogen diffusion front, as shown by the plateau of the carbon concentration curve. This accumulation allows the formation of the alloy carbides, which can transform into alloy nitrides and grain boundary (GB) cementite. The plateau span can be about 100  $\mu\text{m}$ . According to the depth of GB nitrides and the start GB cementite, they are located at relatively higher nitrogen concentrations. Near the surface, decarburization is observed. The longer the nitriding is, the more carbon leaves the surface. As shown, the grey carbon curve for the sample nitrided for 15 hours has a lower carbon concentration at the surface than the other samples nitrided for a shorter time.

Fig.1. (b) shows the hardness profile of these three samples, the effective nitriding depth increases as the nitriding time increases, however, the maximum hardness at the surface does not change very much. Hardening is related to the precipitation of alloying elements nitrides MN (M=Cr, V, Mo...), which are finely dispersed into the ferritic matrix, and thus to the content and diffusion of nitrogen through the treated surface [9], especially in the diffusion zone. So, the more profound the diffusion into the steel in a longer nitriding period, the larger the effective nitriding depth present in the hardness profile. The nitrogen concentration reaches the same limit due to the alloying element concentration in the material, so is the amount of nitride precipitates. Thus, the maximum hardness increment has the same value despite the different nitriding parameters.

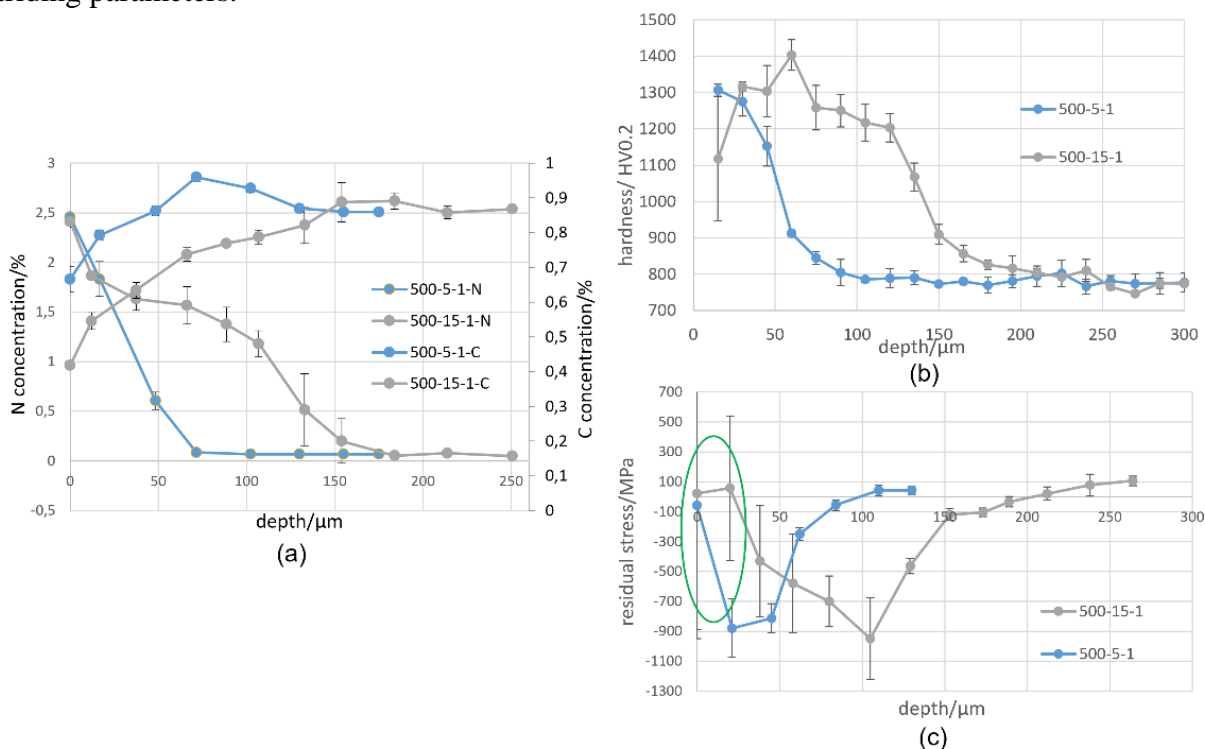


Fig. 1. Surface to an in-depth profile of M2 steel after gas nitriding at 500 °C for 5 and 15 hours with nitriding potential of  $K_N = 1 \text{ atm}^{-1/2}$  (a) N, C profile, (b) hardness profile, (c) residual stress.

Compressive residual stresses are generated due to the positive volumetric eigenstrains accompanying the precipitation of alloying elements nitrides within the ferritic matrix. MN nitrides (M=Cr, V...) are characterized by a higher specific volume than the ferritic matrix (10.7 and 7.1  $\text{cm}^3\text{mol}^{-1}$  respectively) [8,9]. The volume expansion varies depending on the nitrogen fraction. From Fig.1. (c), the maximum compressive residual stress moves to a more profound after nitriding for a longer time, 15 hours. If compared with Fig.1. (a), the maximum residual stress is located just before the carbon plateau. This means that the maximum residual stress

occurs just after the carbon concentration returns to the normal value for the studied M2 steel, accompanied by a transformation from carbides to nitrides at a particular depth. From the phase transformation point of view, all the alloying elements transform into alloy nitrides at the depth where the residual stresses reach the maximum value (if not at the surface). The transformation from initial carbides into nitrides decreases nitriding kinetics and is counteracted by cementite precipitation. This reduces volume change and so residual stresses during nitriding. During nitriding, the evolution of precipitation and phase transformation includes the four steps [9].

- CrN nitrides precipitation occurs at the beginning of the treatment thanks to the high nitrogen affinity, fine semi-coherent CrN nitrides precipitate from solid solution, this generates the first compressive residual stress.

- The transformation from initial carbides to incoherent nitrides offers less volume change due to a minor specific volume difference.

- Diffusion of carbon at the diffusion front: alloying elements form carbides first, then transform to incoherent nitrides, leading the quantity of semi-coherent nitrides to decrease and less volume expansion.

- The transformation from cementite to  $\gamma'$ -Fe<sub>4</sub>N by reacting with the hydrogen in the atmosphere causes decarburization close to the surface, which decreases the elastic loading caused by the prior phase transformation during nitriding.

All the first three steps lead to increased volume and compressive residual stress, with a different ratio. In deeper depths, the second and the third types of phase transformations occur more significantly [10], this leads to less alloying elements joining the first type of phase transformation, which causes the maximum volume expansion among these three. So, when the maximum compressive residual stress occurs in the deeper material, the value usually is less critical than those close to the surface. After the maximum residual stress is reached, like the aging time effect on the precipitate sizes, continuing nitriding leads to the precipitates coarsening and the redistribution of residual stress [11,12]. Surface decarburization involves a reduction in the volume fraction of cementite during nitriding, resulting in surface unloading and thus a reduction in residual stress [8]. After the elastic residual stress is completely balanced out, positive residual stress would be generated (Fig.1. (c) 15 hours nitriding).

### 3.2. Nitriding temperature

Fig.2. shows the chemical and mechanical properties profiles from the surface to in-depths of the M2 samples after nitriding with  $K_N = 0.5 \text{ atm}^{-1/2}$  at temperatures 500 and 540 °C. For both nitrogen and hardness profiles, the values reach the maximum at the surface and gradually decrease until the same as in the core. Lower temperature (500 °C) nitriding leads to less significant hardness increment and lower nitriding depths (effective nitriding depth is defined as the depth where the hardness is 100 HV0.2 higher than that of the base material), as shown in Fig.2.(c). This corresponds to less nitrogen diffusion leading to a low nitride fraction, as shown in Fig.2. (a), less nitrogen concentration in the material from the surface to in-depth than the one nitrided at 540 °C. After carbon enrichment at a certain depth, the carbides transform into nitrides, the cementite precipitate at the grain boundaries. The phase composition allows a maximum volume expansion, and the maximum residual stress occurs. Increase nitriding temperature or nitriding potential or nitriding time, the nitriding layer grows faster, the maximum residual stress occurs in a more profound depth under the surface. In Fig.2. (b), the residual stress shows the highest value at the surface of the sample nitrided at 500 °C, while at about 50  $\mu\text{m}$  in-depth of the sample nitrided at 540 °C due to the residual stress redistribution.

The lower carbon concentration of the sample nitrided at 540 °C (Fig.2. (a)) indicates the more critical decarburization.

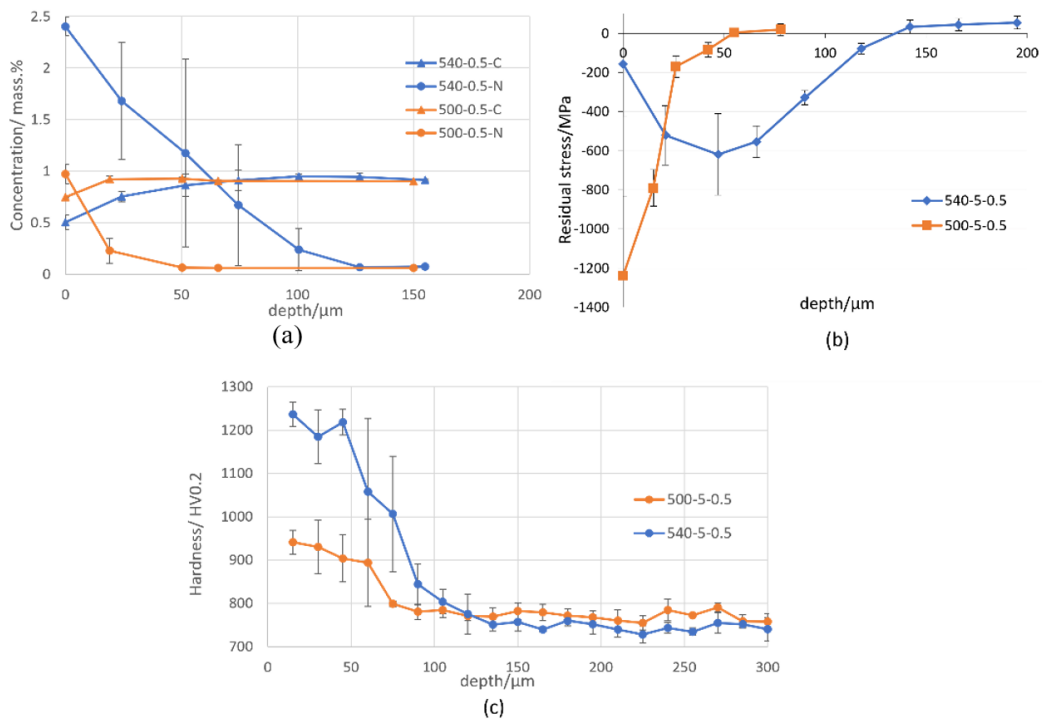


Fig. 2. Surface to an in-depth profile of M2 steel after gas nitriding with  $K_N = 0.5 \text{ atm}^{-1/2}$  at different temperatures (a) N, C profile, (b) residual stress, (c) hardness profile.

### 3.3. Nitriding potential

The N, C profiles, the hardness, and the residual stress profiles in M2 steel samples after gas nitriding at 540 °C are shown in Fig.3. A compound layer is formed with the nitriding potential of  $K_N = 3.7 \text{ atm}^{-1/2}$ , no compound layer for  $0.5 \text{ atm}^{-1/2}$ . Effective nitriding depth is deeper for  $K_N = 3.7 \text{ atm}^{-1/2}$ , so as the depth of the maximum residual stress. These result from the nitrides precipitation, the nitrogen concentration is higher in the sample nitrided with  $K_N = 3.7 \text{ atm}^{-1/2}$ . Higher nitriding potential increases the decomposition of ammonia by increasing the partial pressure of ammonia and providing a higher gradient of nitrogen. This increases the kinetics of diffusion and precipitation. The same reason causes the low residual stress and low carbon concentration near the surface explained earlier, carbon co-diffusion induced by the transformation from carbides into nitrides, causes the volume of the precipitates to decrease at the surface.

## 4. Conclusion

The nitrogen concentration gradient is created during nitriding as the maximum is at the surface. The hardness gradient is generally inconsistent with the nitrogen concentration. However, the residual stress redistributes when nitriding is longer than a specific time due to the precipitates coarsening and the multiple phase transformations. The maximum residual stress is generally located at the end of the hardness plateau in the in-depth profile and at the nitrogen diffusion front, deeper than that, carbon accumulation can be observed. But in terms of nitriding time and phase evolution, the maximum residual stress occurs after the carbides transformation and carbon co-diffusion to form new carbides. The residual stress at the surface decreases after reaching the maximum due to decarburization.

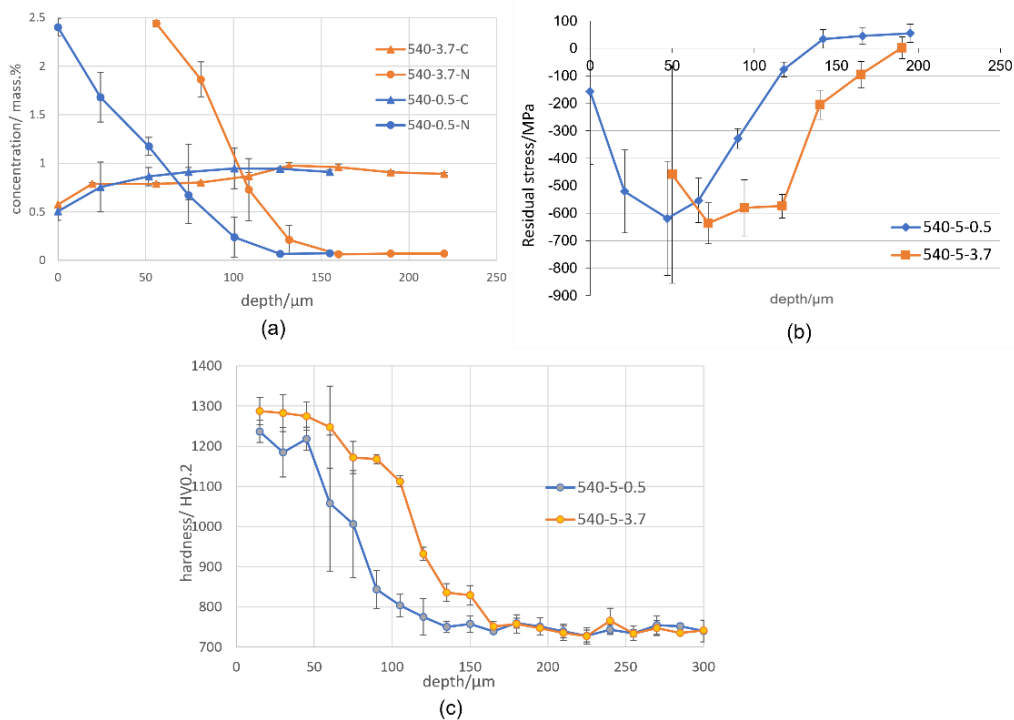


Fig. 3. Surface to an in-depth profile of M2 steel after gas nitriding at 540 °C with different nitriding potential (a) N, C profile, (b) residual stress, (c) hardness profile.

## References

- [1] L.H.P. Abreu, M.C.L. Pimentel, W.F.A. Borges, T.H.C. Costa, M. Naeem, J. Iqbal, and R.R.M. Sousa. Plasma nitriding of AISI M2 steel: performance evaluation in forming tools. *Surface Engineering*, p.1-8, 2020.
- [2] I. Hacısalihoglu, F. Yildiz, and A. Alsaran. Wear performance of different nitride-based coatings on plasma nitrided AISI M2 tool steel in dry and lubricated conditions. *Wear*, 384(2017)159-168.
- [3] R. Mohammadzadeh, A. Akbari, and M. Drouet. Microstructure and wear properties of AISI M2 tool steel on RF plasma nitriding at different N<sub>2</sub>-H<sub>2</sub> gas compositions. *Surface and Coatings Technology*, 258(2014)566-573.
- [4] E.J. Mittemeijer, *Fundamentals of nitriding and nitrocarburizing*, ASM International, 153(2013)619-646.
- [5] E.J. Mittemeijer and M.A.J. Somers. Thermodynamics, kinetics, and process control of nitriding. *Surface Engineering*, 13(6):483-497, 1997.
- [6] S. Jégou, R. Kubler and L. Barrallier, On residual stresses development during nitriding of steel: thermochemical and time dependence, *Advanced Materials Research Vols. 89-91 (2010) pp 256-261*
- [7] L. Barrallier, J. Barrallis, On origin of residual stresses generated by nitriding treatment on alloy steel. *Proc. 4th Int. Conf. Residual Stress, Baltimore. (1994), p.498-505*
- [8] S. Jégou, L. Barrallier, and G. Fallot, Gaseous nitriding behavior of 33CrMoV12-9 steel: Evolution of the grain boundaries precipitation and influence on residual stress development. *Surface and Coatings Technology*, 339(2018)78-90.
- [9] S. Jégou, L. Barrallier, and R. Kubler. Phase transformations and induced volume changes in a nitrided ternary Fe-3%Cr-0.345%C alloy. *Acta Materialia*, 58(7):2666- 2676, 2010.

- [10] S. Jegou, L. Barrallier, R. Kubler, and M.A.J. Somers. Evolution of residual stress in the diffusion zone of a model Fe-Cr-C alloy during nitriding. *HTM Journal of Heat Treatment and Materials*, 66(3):135–142, 2011.
- [11] Van Landeghem, P. Hugo, M. Gouné, and A. Redjaïmia, (2012). Nitride precipitation is compositionally heterogeneous alloys: Nucleation, growth, and coarsening during nitriding. *Journal of crystal growth*, 341(1), 53-60.
- [12] T. Steiner, M. Akhlaghi, S.R. Meka, and E.J. Mittemeijer, (2015). Diffraction-line shifts and broadenings in continuously and discontinuously coarsening precipitate-matrix systems: coarsening of initially coherent nitride precipitates in a ferrite matrix. *Journal of materials science*, 50(21), 7075-7086.